

Study on flotation behavior and mechanism of separating chalcopyrite and Molybdenite with ethyl mercaptoglycolate as inhibitor

Xiao-Feng Yang, Xu-Zhao, Yao-Yao Liu

Heilongjiang University of Science and Technology School of Mining Engineering

Corresponding author: yangxiaofeng82@sina.com (Xiao-Feng Yang)

Abstract: The effect of ethyl thioglycolate organic small molecule inhibitors on chalcopyrite molybdenite flotation behaviour is investigated via single mineral micro-flotation tests, zeta potential tests, and X-ray photoelectron spectroscopy (XPS) analysis. Results of the flotation test indicate that ethyl thioglycolate organic small-molecule inhibitors can effectively separate Cu and Mo and selectively inhibit chalcopyrite under weak alkaline conditions. Infrared spectroscopy and XPS analysis show that hydrophilic functional groups C=O and -COOH in the ethyl thioglycolate organic small molecules can chemically adsorb onto the chalcopyrite surface. Moreover, ethyl thioglycolate has no obvious effect on zeta potential of molybdenite. Therefore, ethyl thioglycolate can effectively separate chalcopyrite and molybdenite.

Keywords: ethyl thioglycolate, chalcopyrite, molybdenite, inhibitor, separation

1. Introduction

Cu and Mo are important metal resources that are widely used in military and manufacturing fields (Zeng, 2012; Zang, 2017). Porphyry Cu–Mo ore is the main resource for extracting Cu and Mo (Song et al., 2012). Currently, three main methods are widely used in the recovery of Cu and Mo sulphide ore (Ansari and Pawlik, 2007; Lin et al., 2017; Yin et al., 2017), as follows: 1) Mixed flotation – first, useful metal minerals Cu and Mo are floated together to obtain a mixed concentrate. Next, Cu and Mo are separated from the mixed concentrate to obtain Cu and Mo concentrates; 2) Preferential flotation – a flotation process in which Cu or Mo is preferentially floated and the remaining mineral is activated to float another mineral; 3) Equal flotation – also known as the separate mixed flotation method, which can not only pharmaceutical consumption, but also improve the flotation index. In the actual production of a concentrator, an inhibitor is typically incorporated to increase the difference between the floatability of Cu and Mo to separate Cu and Mo. Sodium sulphide, Sodium hydrosulphide, and Knox agents are widely used in industrial production (Qiu and Dai, 2009; Yin et al., 2010; Liu, 2012). However, they are used in high amounts owing to their inferior stability. The various chemical behaviours of sodium sulphide and sodium hydrosulphide in the pulp will produce toxic hydrogen sulphide gas, which not only endangers the physical and mental health of the staff, but also causes pollution to the environment (Huang et al., 2019).

In recent years, with the continuous development of Cu-Mo concentrate separation technology worldwide, researchers are paying more and more attention to the study of organic inhibitors. Xanthan gum, a polymer polysaccharide, is a degradable and environmentally friendly inorganic inhibitor, which can replace or surpass the traditional inhibitors as a new molybdenum inhibitor in Cu-Mo sulfide ore (Yan et al., 2020). Some studies show that xanthan gum also has obvious inhibitory effect on sphalerite (Feng et al., 2020). The non-toxic, environmentally friendly, naturally degradable carboxymethyl chitosan has a strong inhibition effect on Mo, but has no significant effect on chalcopyrite flotation. It is also a new molybdenum inhibitor with good selectivity and inhibition effect (Yuan et al., 2019). In addition, it has been found that humic acid can selectively inhibit Mo in the flotation separation of copper and molybdenum in a wide range of pH (Yuan et al., 2019). In contrast, in terms of chalcopyrite inhibitors, DMSA, which is often used as an antidote for heavy metals, shows excellent inhibition effect

on chalcopyrite, and low dose of DMSA can effectively inhibit chalcopyrite in a large pH range (Li et al., 2015).

Ethyl thioglycolate is a low-cost organic small molecule compound. The main functional groups are carboxyl and carbonyl groups (He et al., 2013). In this study, the effect of ethyl thioglycolate on chalcopyrite molybdenite flotation behaviour is investigated, and the inhibition mechanism of ethyl thioglycolate on chalcopyrite is investigated via micro-flotation, zeta potential tests, and X-ray photoelectron spectroscopy (XPS) analysis to provide a theoretical basis for the flotation separation of Cu and Mo.

2. Materials and methods

2.1. Materials and reagents

For the experiment, chalcopyrite was obtained from the natural chalcopyrite of Dexing Cu Mine in China, and molybdenite was obtained from the natural molybdenite of Yichun Luming Mining Co., Ltd. Achieve a grain size of 38~74 μm . Samples with particle size of 74 μm were used for the flotation test. The results are shown in Fig. 1(a) and (b). Fig. 1 shows that chalcopyrite and molybdenite contained few impurities and are of high purity. ICP was used to analyse the chemical elements of a single mineral. The results showed that the grade of chalcopyrite single mineral was 37.21% and its purity was 93.65%. Meanwhile, the grade of molybdenite single mineral was 56.02% and its purity was 97.21%. -74 μm samples were used for flotation tests and -38 μm samples were used for X-ray diffraction, potentiodynamic testing, infrared spectroscopy, and X-ray photoelectron spectroscopy.

Ethyl thioglycolate was compounded synthesised by the Key Laboratory of Mineral Processing, Heilongjiang University of Science and Technology. Collector butyl xanthate and foaming agent methyl isobutyl methanol (MIBC) (Weifang Jiahua Chemical Co., Ltd.) of analytical grade were used. Hydrochloric acid and solid flake sodium hydroxide (Tianjin Zhiyuan Chemical Reagent Co., Ltd.) of analytical grade were used to adjust the pH value of the pulp. The water used for the test was high-purity water (temperature = 26 °C; resistivity = 18.00 M Ω -cm).

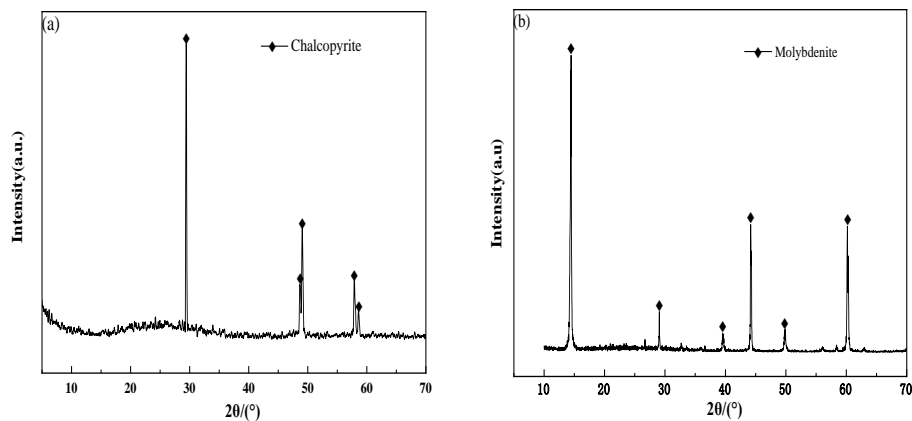


Fig. 1. (a) X-ray diffraction pattern of chalcopyrite; (b) X-ray diffraction pattern of molybdenite

2.2. Single mineral flotation test

An XFG-1600 flotation machine (mechanical agitation) with a volume of 40 mL (Changsha Prospecting Machinery Factory, China) was used in the flotation tests. Pure minerals (2 g) with a particle size of 0.074 mm were placed in a 100 mL beaker containing 80 mL of high-purity water. After ultrasonic treatment for 5 min and standing for 30 min, the supernatant was removed. The treated ore samples were immediately transferred to a flotation tank, and a hanging trough micro-flotation machine was operated. The rotation speed of the flotation machine was set to 1549 rpm to agitate the slurry evenly. Hydrochloric acid and sodium hydroxide solutions prepared in advance were used to adjust the pH of the slurry required for the test. The inhibitor ethyl thioglycolate (5 min), collector butyl xanthate (2 min), and foaming agent MIBC (2 min) were added to the slurry in sequence, and the baffle was adjusted such that it was inflated. After the foam layer on the slurry surface stabilised, flotation scraping was started,

and flotation was performed for 3 min. At the end of the flotation, the flotation foam and products in the tank were obtained, dried, and weighed.

2.3. Mixed mineral flotation test

A mixed ore comprising chalcopyrite and molybdenite was prepared by mixing chalcopyrite and molybdenite (mass ratio of 1:1). Based on the operation steps of single-mineral flotation, the speed was adjusted to 1549 rpm, and the flotation time was set to 3 min. The concentrate and tailings obtained after the flotation were obtained, dried, weighed, and tested to calculate the recovery rate.

2.4. Zeta potential measurement

A 1 g sample with a particle size of 0.045 mm was placed into a 50 mL beaker containing 30 mL of high-purity water and then stirred evenly using a magnetic stirrer. HCl and NaOH solutions were used to adjust the pH value required to measure the zeta potential of the slurry. A certain amount of ethyl thioglycolate was added, and the pulp was immediately transferred to the potential test tank of a JS94H microelectrophoresis apparatus (Shanghai Zhongchen Digital Technology Equipment Co., LTD) for analysis. To ensure the accuracy of the results, each sample was tested four times, and the average of the results was obtained.

2.5. FTIR measurement

A 1.5 g of the sample was placed in a 100 mL Erlenmeyer flask containing 50 mL of high-purity water; subsequently, a certain amount of ethyl thioglycolate inhibitor was added. The Erlenmeyer flask was placed in a SHY-2A (Jiangsu Jintan Jincheng Guosheng Experimental Instrument Factory) constant-temperature water-bath shaker, the rotation speed was adjusted to 194.80 r/min, and the flask was shaken for 1 h. Subsequently, the sample was cleaned three times with high-purity water, filtered using a SHY-DIII (Jintan Youlian Instrument Research Institute) circulating water multi-purpose vacuum pump, dried at a low temperature, placed into the sample bag, and labelled for infrared spectroscopy. Next, 1–2 mg of the solid sample was mixed evenly with 200 mg of pure potassium bromide and ground until the particle size was less than 2 μm . The solid sample was pressed into transparent flakes on a tablet press for analysis. Subsequently, liquid samples were deposited onto a pressed potassium bromide sheet for analysis.

2.6. X-ray photoelectron spectroscopy analysis

The samples tested in this experiment were analysed via XPS using a PHI 5700 ESCA System X-ray photoelectron spectrometer (Physical Electronics Corporation, America). The acceleration voltage and the applied current were 40 kV and 25 mA, respectively. The binding energy (B.E.) scale was calibrated from the carbon contamination (always present at the material surface) using the C1s peak at 284.8 eV.

3. Results and discussion

3.1. Mineral flotation test

Fig. 2 (a) shows the effect of pH (2~10) on the floatability of chalcopyrite and molybdenite in the presence and absence of ethyl petrol thioglycolate. In the entire single-mineral flotation process, the amount of butyl xanthate as the collector was 20 ppm, and the amount of MIBC as the foaming agent was 20 ppm. Fig. 2 (a) shows that chalcopyrite and molybdenite exhibited similar floatability variation trends with the change in the slurry pH (2~10), which further proves that the effective separation of Cu and Mo must be accomplished by adding additional inhibitors. When the pH of the pulp was between 2 and 8, the recoveries of molybdenite and chalcopyrite increased slightly. When the pH of the pulp was 8, the recoveries of molybdenite and chalcopyrite reached the maximum values of 95.28% and 95.97%, respectively, which is consistent with the results reported in previous publications (Li et al., 2015). The dose of the ethyl thioglycolate inhibitor was fixed at 17.5 ppm. The effect of pH on the floatability of molybdenite and chalcopyrite in the presence of ethyl thioglycolate was investigated. As shown in Fig. 2 (a), the recovery rate of molybdenite was similar to that without the addition of ethyl

thioglycolate inhibitors. The recovery rate of chalcopyrite decreased when the pulp pH ranged from 2 to 8. When the pulp pH was 8, the recovery rate of chalcopyrite was only 5.35%, which was its minimum value, and the effective separation of Cu and Mo was realised.

Results from the dosage test of Cu inhibitor ethyl thioglycolate under the optimal pH 8 slurry condition, as shown in Fig. 2 (b), were analysed. As shown in Fig. 2 (b), the recovery rate of chalcopyrite decreased significantly as the amount of Cu inhibitor ethyl thioglycolate continued to increase, whereas the floatability of molybdenite was relatively high and unaffected by the Cu inhibitors. This indicates that the pharmaceutical may be adsorbed on the surface of chalcopyrite but not on the surface of molybdenite, which further verifies the good selectivity of inhibitor ethyl thioglycolate and the inhibition effect on Cu.

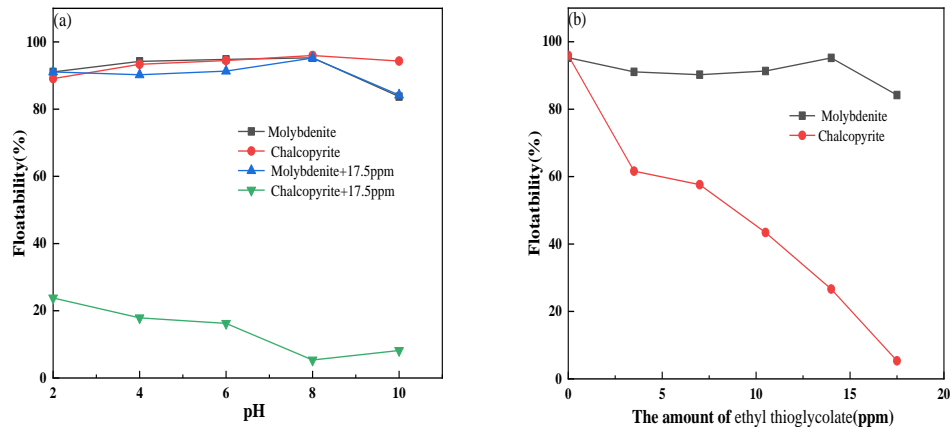


Fig. 2. (a) The influence of pH on the floatability of different minerals; (b) The influence of the amount of ethyl thioglycolate on the floatability of different minerals.

3.2. Zeta potential

Fig. 3 shows the effect of ethyl thioglycolate before and after adsorption on the chalcopyrite and molybdenite surface potential with the change in pH. Fig. 3 shows that the surface potential of molybdenite was negatively charged over a wide pH range; after the addition of pharmaceutical ethyl petrol thioglycolate, the surface potential of molybdenite did not change significantly, which verified the flotation behaviour, in which the recovery rate of molybdenite remained almost unchanged at different pH values. When chalcopyrite was not treated by ethyl petrol thioglycolate, its equipotential pH value was 5, which is consistent with previous reports (Mitchell et al., 2004). When the pH exceeded 5, the chalcopyrite surface was negatively charged. When ethyl thioglycolate was added, chalcopyrite maintained a negative potential over a wide pH range (pH = 2–10), but the absolute value of its potential increased, indicating that ethyl thioglycolate was adsorbed on the surface of chalcopyrite.

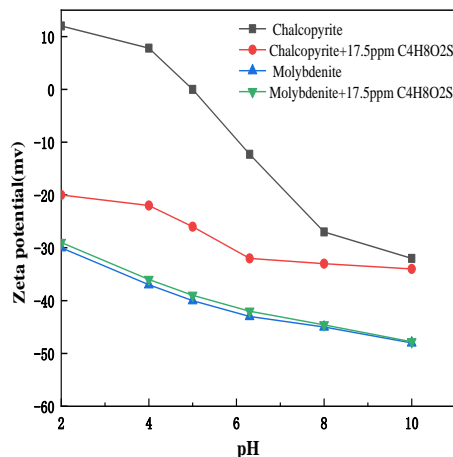


Fig. 3. Effect of pH on zeta potential on the surface of different minerals

3.3. FTIR analysis

Fig. 4 shows the IR spectra of inhibitor ethyl thioglycolate and the IR spectra of chalcopryrite and molybdenite before and after treatment with ethyl petrol thioglycolate. Fig. 4 (a) shows the IR spectra of chalcopryrite before and after treatment with the ethyl thioglycolate inhibitor. As shown in Fig. 4 (a), in the wavelength range of 900–1800 cm^{-1} , a new stretching vibration appeared at wavenumbers 1655, 1569, 1388, and 1044 cm^{-1} ; these new absorption peaks belonged to the inhibitor ethyl thioglycolate molecules, which further indicates that ethyl thioglycolate can be adsorbed on the surface of chalcopryrite. Based on the literature (Rath et al., 2000; Zheng et al., 2019), the stretching vibrations at 1655, 1569, 1388, and 1044 cm^{-1} belonged to the double bond C=O stretching vibration in the carboxyl group, C=C stretching vibration, C-H stretching vibration absorption peak of methylene, and C-O stretching vibration peak, respectively. It was further verified that the carboxyl carbonyl groups in the ethyl thioglycolate organic small molecule inhibitors can be selectively adsorbed on the chalcopryrite surface, but not on the molybdenite surface.

As shown in Fig. 4 (b), the IR spectra for the surface of high-purity molybdenite, before and after the action of inhibitor ethyl petrol thioglycolate, did not change significantly, indicating no physical or chemical adsorption of ethyl thioglycolate on the surface of molybdenite. This further verifies that the floatability of molybdenite was unaffected by the inhibitor.

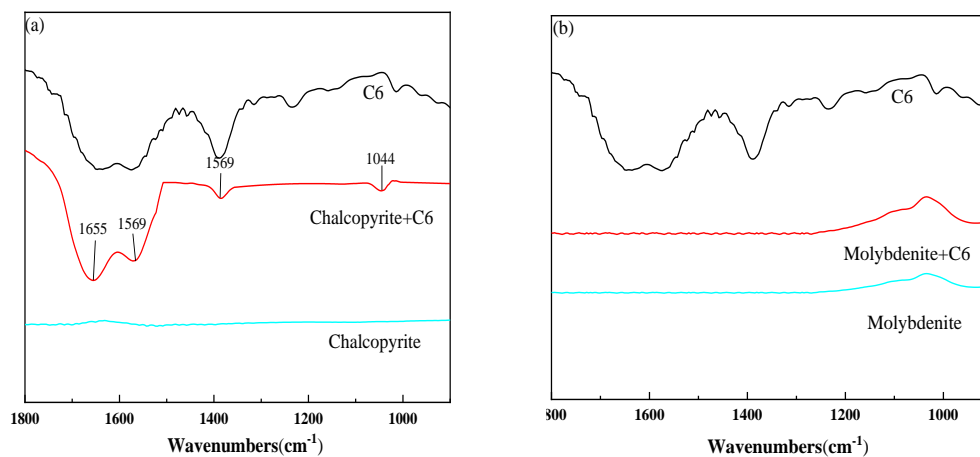


Fig. 4. (a) Infrared spectra of ethyl thioglycolate and chalcopryrite before and after treatment with ethyl petrol thioglycolate; (b) Infrared spectra of ethyl thioglycolate and molybdenite before and after treatment with ethyl petrol thioglycolate

3.4. XPS analysis

XPS is an important surface analysis technique. It not only provides information regarding the molecular structure and valence state for chemical investigation, but also information regarding the elemental composition, chemical state, and molecular structure of various compounds for electronic material investigation. Fig. 5 shows a full spectrum scan of chalcopryrite treated and untreated with agent ethyl petrol thioglycolate. The scan range of the full spectrum was 0~1200eV. As shown in Fig. 5, prior to the adsorption of ethyl thioglycolate, chalcopryrite contained elements Cu, Fe, O, C, and S on its surface, among which O appeared because of the oxidation of the chalcopryrite surface. Changes in the relative concentration of each element are presented in Table 1. As shown, the relative concentration of C in chalcopryrite treated with the ethyl thioglycolate inhibitor increased by 6.71%, which was primarily caused by two factors: the introduction of organic carbon to the operation analysis, and the introduction of element C to chalcopryrite treated with the ethyl thioglycolate agent. The decreased in the Cu and S atomic concentrations by 0.24% and 4.61%, respectively, indicates that adsorption occurred between ethyl thioglycolate and the chalcopryrite surface.

Fig. 6 shows the C1s spectra of the chalcopryrite surface in the presence and absence of ethyl petrol thioglycolate. As shown in Fig. 6, the peak values of the C1s map of chalcopryrite without ethyl thioglycolate treatment were 284.80 and 286.00eV, respectively. The changed of characteristic peak of

chalcopyrite indicates that ethyl thioglycolate may be chemically adsorbed on chalcopyrite surface. A new characteristic peak appeared in the C1s spectra of the chalcopyrite surface treated with ethyl thioglycolate agent, and its binding energy was 288.20eV (C=O). The increased in the carbon atomic concentration, as presented in Table 1, indicates that the organic inhibitor ethyl thioglycolate molecules can coat the surface of chalcopyrite, which is consistent with the results of the micro-flotation test and infrared spectrum analysis. It was further verified that chalcopyrite can be selectively inhibited by ethyl thioglycolate agents.

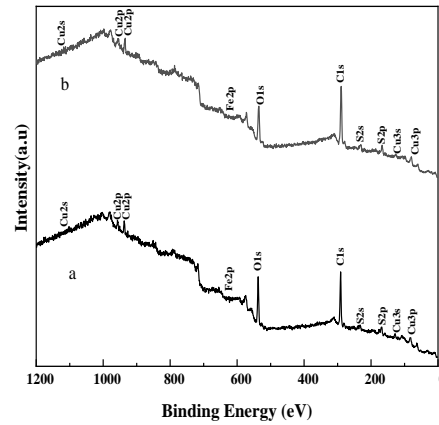


Fig. 5. Full spectrum scan of chalcopyrite surface before and after ethyl thioglycolate adsorption

Table 1. Surface partial atomic concentration of chalcopyrite

Sample analysis	Atomic concentration		
	C1s	Cu2p	S2p
chalcopyrite	60.60	2.08	10.04
chalcopyrite+ethyl petrol thioglycolate	67.31	1.84	5.43

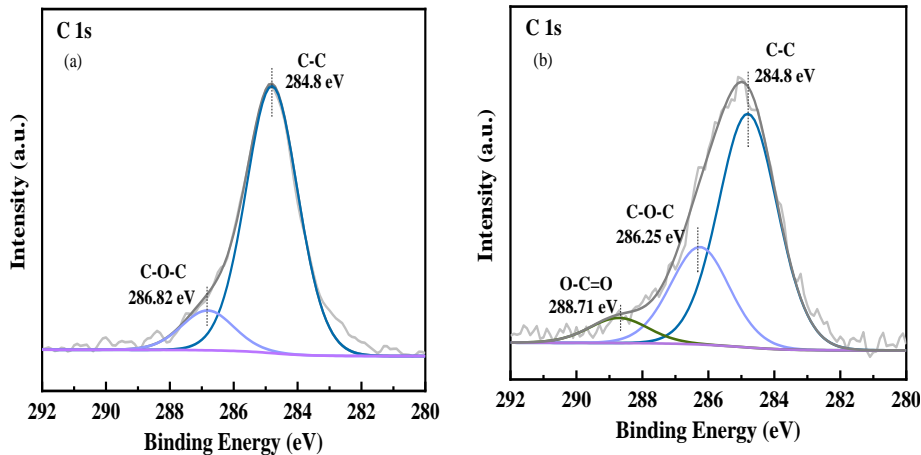


Fig. 6. Narrow spectrum of carbon in chalcopyrite before(a) and after(b) treatment with ethyl petrol thioglycolate

The narrow spectrum of S before and after chalcopyrite treatment with inhibitor ethyl thioglycolate is shown in Fig. 7. Fig. 7 (a) shows the drug adsorption of single-mineral chalcopyrite in a narrow area S2p scanning atlas, where characteristic peaks appeared at binding energies of 161.73, 162.84, 163.90, 165.20 and 169.05eV. The double peaks at 161.73, 162.84, 163.90, 165.20, 169.05 and 170.35eV corresponded to the S2p orbitals, which were S2-, S22-, and SO42- respectively. The results indicate that S appeared primarily on the chalcopyrite surface in the form of CuS and Cu2S, whereas some S elements

were oxidised. The spectrum of S on the surface of chalcopyrite after it was subjected to agent ethyl thioglycolate is shown in Fig. 7 (b). The positions of the characteristic absorption peaks of S²⁻- and S²²⁻-lowered, indicating that ethyl thioglycolate was adsorbed by reacting with CuS and Cu₂S on the surface of chalcopyrite, resulting in a decrease in the relative concentration of S atoms. Compared with the chalcopyrite before treatment with the chemical, the characteristic peaks at binding energies 169.05 and 170.35 eV disappeared, which further shows that ethyl thioglycolate adsorbed on the surface of chalcopyrite and .

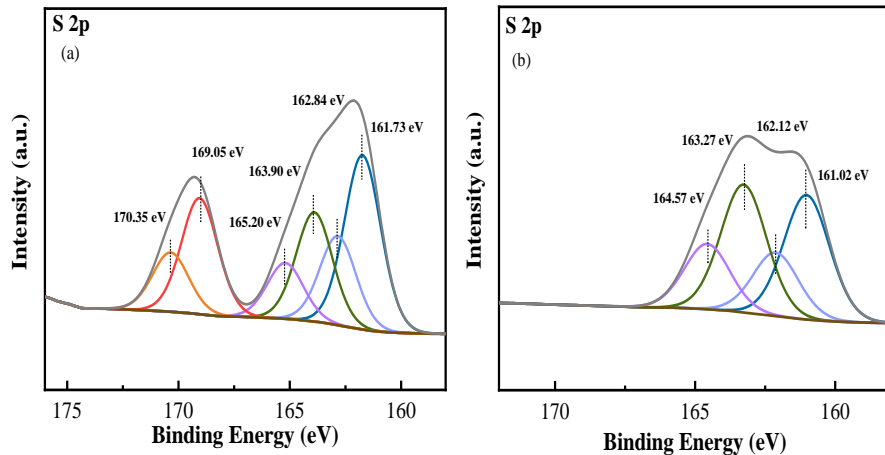


Fig. 7. Narrow spectrum of sulfur in chalcopyrite before(a) and after(b) treatment with ethyl petrol thioglycolate

Fig. 8 shows the XPS narrow-area scan spectrum of Cu on the surface of chalcopyrite. As shown in Fig. 8(a), for the chalcopyrite prior to ethyl thioglycolate treatment, the binding energies of the narrow-area scanning spectrum of Cu₂p were 932.93 and 952.85 eV, which were the binding energies at which the characteristic peaks of chalcopyrite appear. Meanwhile, 935.83 and 955.47 eV were the binding energies of the Cu(OH)₂ 2p_{3/2} and 2p_{1/2} orbitals, respectively. After adding the ethyl thioglycolate inhibitor, the binding energy of CuFeS₂ increased from 932.93 to 935.38 eV, and the bond energy at 954.78 eV increased to 954.78 eV. The decreased in the electron cloud density was due to the transfer of electrons, likely from the Cu atoms to the S atoms. The binding energies of the Cu(OH)₂ 2p_{3/2} and 2p_{1/2} orbitals at 935.83 and 955.47 eV decreased to 933.31 and 952.8 eV, respectively, and their electron density increased. This phenomenon was attributed to the chemical adsorption of ethyl thioglycolate and Cu(OH)₂ due to natural oxidation on the surface of chalcopyrite.

Fig. 9 shows the XPS narrow-area scan of Fe on the surface of chalcopyrite before and after treatment with inhibitor ethyl petrol thioglycolate. As shown in Fig. 9, in addition to the characteristic peak of chalcopyrite when agent ethyl thioglycolate was not involved, a characteristic peak of (-OOH) FeOOH

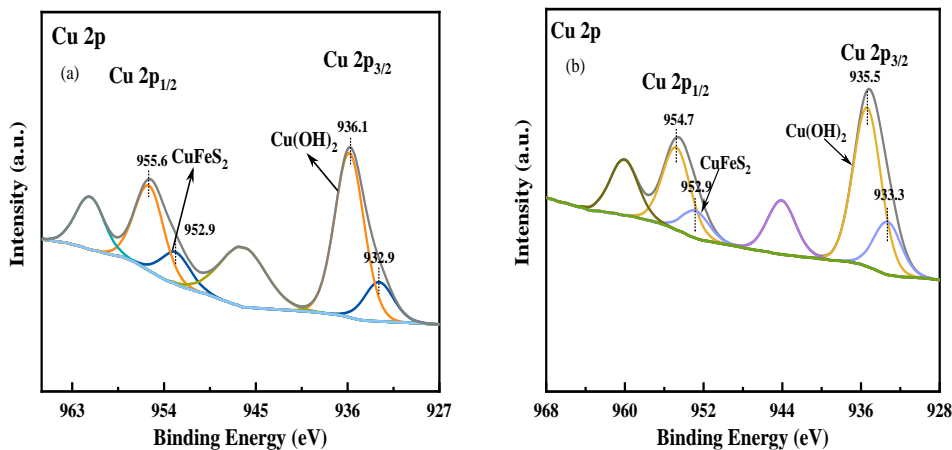


Fig. 8. Narrow spectrum of copper in chalcopyrite before(a) and after(b) treatment with ethyl petrol thioglycolate

appeared at the binding energy of 711.5eV, indicating that some of the iron may had been oxidized. After the action of agent ethyl petrol thioglycolate, the intensity of the characteristic peak at binding energy 711.5eV increased, which further proved that the surface wettability of chalcopyrite in the slurry increased.

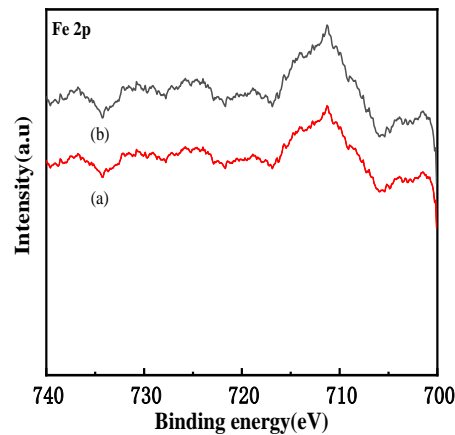


Fig. 9. Narrow spectrum of iron in chalcopyrite before(a) and after(b) treatment with ethyl petrol thioglycolate

4. Conclusions

In this study, the effect of ethyl thioglycolate organic small molecule inhibitors on the floatability of molybdenite and chalcopyrite, as well as the mechanism of the ethyl thioglycolate organic small molecule inhibitor in inhibiting chalcopyrite are investigated. The main conclusions are as follows:

(1) In an environment with a weak base (pH = 8), the ethyl thioglycolate organic small molecule inhibitor do not impose an inhibitory effect on molybdenite. However, at a certain dosage, the ethyl thioglycolate organic small molecule inhibitor could selectively inhibit chalcopyrite and effectively separate Cu and Mo.

(2) The zeta potential test further shows that the ethyl thioglycolate organic small molecule inhibitor imposed an adsorption effect on the surface of chalcopyrite, without any interaction with the surface of molybdenite.

(3) The ethyl thioglycolate organic small-molecule inhibitors contained hydrophilic functional groups, such as C=O and -COOH. FTIR and XPS test results shows that hydrophilic functional groups such as carbonyl and carboxyl groups can be firmly adsorbed on the surface of chalcopyrite in the form of chemical adsorption, thereby affording the effective inhibition of chalcopyrite.

Acknowledgments

Thanking for the support of national natural science foundation of China and Heilongjiang Provincial Department of Education.

References

- ANASARI, A., PAWLIK, M., 2006, *Floatability of chalcopyrite and molybdenite in the presence of lignosulfonates*. Part ii. Hallimond tube flotation. *Minerals Engineering*, 20(6), 609-616.
- FENG, B., GUO, Y.T., WANG, T., PENG, J.X., NING, X.H., WANG, H.H., 2020, *Role and mechanism of xanthan gum in flotation separation of chalcopyrite and sphalerite*. *Chinese Journal of Nonferrous Metals*, 30(05), 1202-1208.
- HE, W., ZHOU, G., LIU, L., 2013, *New synthesis process and application of ethyl thioglycolate*. *Modern Mining*, 29(11), 17-20.
- HUANG P.L., YANG B.Q., HU Y.J., YAN H., TENG A.P., 2019, *Research progress of Cu-Mo separation technology*. *Nonferrous Metals (Mineral Processing)*, 05, 50-55. (in Chinese)
- LI, M.Y., WEO, D.Z., LIU, Q., LIU, W.B., SUN, H.J., 2015, *Flotation separation of copper-molybdenum sulfides using chitosan as a selective depressant*. *Minerals Engineering*, 83, 217-222.

- LI, M.Y., WEI, D.Z., SHEN, Y.B., LIU, W.G., GAO, S.L., LIANG, G.Q., 2015, *Selective depression effect in flotation separation of copper–molybdenum sulfides using 2,3-disulfanylbutanedioic acid*. Transactions of Nonferrous Metals Society of China, 25(9), 3126-3132.
- LIN, Q.Q., GU, G.H., WANG, H., LIU, Y.C., 2017, *Recovery of molybdenum and copper from porphyry ore via iso-flotability flotation*. Transactions of Nonferrous Metals Society of China, 2260-2271.
- LIU, G.Y., LU, Y.P., ZHONG, H., CAO, Z.F., XU, Z.H., 2012, *A novel approach for preferential flotation recovery of molybdenite from a porphyry copper–molybdenum ore*. Minerals Engineering, 36-38.
- MITCHELL, T.K., NGUYEN, A.V., EVANS, G.M., 2004, *Heterocoagulation of chalcopyrite and pyrite minerals in flotation separation*. Advances in Colloid and Interface Science, 114-115, 227-237.
- QIU, L.N., DAI, H.X., 2009, *Flotation process and recent reagents status of molybdenum ore*. Modern Mining, vol. 22-23.
- RATH, R.K., SUBRAMANIAN, S., PRADEEP, T., 2000, *Surface chemical studies on pyrite in the presence of polysaccharide-based flotation depressants*. Journal of Colloid and Interface Science, 229(1), 82-91.
- SONG, S.X., ZHANG, X.W., YANG, B.Q., 2012, *Flotation of molybdenite fines as hydrophobic agglomerates*. Separation and Purification Technology, 98, 451-455.
- YAN, H., YANG, B., ZENG, M., HUANG, P., TENG, A., 2020, *Selective flotation of Cu-Mo sulfides using xanthan gum as a novel depressant*. Minerals Engineering, 156.
- YIN, W.Z., ZHANG, L.R., and XIE, F., 2010, *Flotation of Xinhua molybdenite using sodium sulfide as modifier*. Transactions of Nonferrous Metals Society of China, 20(4), 702-706.
- YIN, Z.G., SUN, W., HU, Y.H., GUAN, Q.J., ZHANG, C.H., GAO, Y.S., ZHAI, J.H., 2017, *Depressing behaviors and mechanism of disodium bis (carboxymethyl) trithiocarbonate on separation of chalcopyrite and molybdenite*. Transactions of Nonferrous Metals Society of China, 27(4), 883-890.
- YUAN, D., CADIEN, K., LIU, Q., ZENG, H., 2019, *Flotation separation of Cu-Mo sulfides by O-carboxymethyl chitosan*. Minerals Engineering, 2019, 134, 202-205.
- YUAN, D., CADIEN, K., LIU, Q., ZENG, H., 2019, *Selective separation of copper–molybdenum sulfides using humic acids*. Minerals Engineering, 133, 43-46.
- ZANG, C., 2017, *Research on the new inhibitor of sulfide copper–molybdenum mine and its mechanism*. Jiangxi University of Science and Technology, China.
- ZENG, J.M., 2012, *Selective flotation and first-principles study on copper–molybdenum ore*. Center South University, China.
- ZHENG, M.X., LIAN, F.L., XIONG, Y., LIU, B., ZHU, Y.J., MIAO, S., ZHANG, L.T., ZHENG, B.D., 2019, *The synthesis and characterization of a xanthan gum-acrylamide-trimethylolpropane triglycidyl ether hydrogel*. Food Chemistry, 272, 574-579.